Crystals 2022

MDPI

Type of the Paper (Proceedings, Abstract, Extended Abstract, Editorial, etc.)

Effects of Cu, K and guanidinium addition to $CH_3NH_3PbI_3$ perovskite solar cells

Ayu Enomoto [1], Atsushi Suzuki [1,*], Takeo Oku [1], Masanobu Okita [2], Sakiko Fukunishi [2], Tomoharu Tachikawa [2], and Tomoya Hasegawa [2,]

[1] Department of Materials Science, The University of Shiga Prefecture, 2500 Hassaka, Hikone, Shiga 522-8533, Japan; oe21aenomoto@ec.usp.ac.jp (A.E.); oku@mat.usp.ac.jp (T.O.)
[2] Osaka Gas Chemicals Co., Ltd., 5-11-61 Torishima, Konohana-ku, Osaka 554-0051, Japan; okita@ogc.co.jp (M.O.); fukunishi@ogc.co.jp (S.F.); t-tachikawa@ogc.co.jp (T.T.); hasegawa_tomoya@ogc.co.jp (T.H.)
* Correspondence: suzuki@mat.usp.ac.jp (A.S.); Tel.: +81-749-28-8369
† Presented at the

Abstract: Fabrication and characterization of $CH_3NH_3PbI_3$ perovskite solar cell with addition of copper (Cu), and potassium (K) or guanidinium (GA) was performed. Additive effects on the photovoltaic properties, morphologies and crystalline structures were investigated by the experimental results, and electronic structures and thermodynamic stabilities. The stability and conversion efficiency of the perovskite solar cells was improved by incorporating Cu at the lead site, and K or GA at the organic cation, CH_3NH_3, at A-site in cubic crystal. The simultaneous addition of Cu and K to the perovskite crystal suppressed the crystal decomposition while inhibiting desorption of MA, improving the stability of the performance.

Keywords: perovskite; solar cell; polysilane; decaphenylcyclopentasilane; photovoltaic device; copper; guanidinium; potassium

Citation: Lastname, F.; Lastname, F.; Lastname, F. Title. *Chem. Proc.* **2021**, *3*, x. https://doi.org/10.3390/xxxxx

Published: date

1. Introduction

The semiconductor lead halide perovskite (LHP) attracted attention as the active layer of LEDs in the 1990s, and in the 2000s it was rapidly developed as the thin-film absorber layer of solar cells, and has been actively researched worldwide [1]. There is also a growing number of computational simulation works [2-6]. Although perovskite solar cells (PSC) have the advantage of being inexpensive to produce, they have serious problems of low durability and environmental pollution by Pb [7]. The durability of PSC is caused mainly by the decomposition of the perovskite crystals due to methylammonium (MA) desorption. To solve these problems, attempts to improve the interface of perovskites and to introduce additives into the perovskite layer to improve the electronic properties have been studied [8-11]. Previous studies have reported that substitution of guanidinium (GA), which is larger than MA, can inhibit MA desorption, resulting in improved performance and long-term stability [12-15]. In addition, it has been reported that potassium (K) addition improves the electron transport layer (ETL) and perovskite interface state [16-19]. It has also been reported that the addition of environmentally benign transition metals other than Pb reduces toxicity and changes the electronic state to improve the performance of PSC [20-23]. Among them, the environmentally friendly transition metal Cu has been considered as a candidate for Pb replacement, but there are few reported cases [24-28].

The aim of this work is to fabricate and characterize devices doped with Cu, GA and K. The photovoltaic properties, morphologies and crystal structure were investigated by substitution of Cu, GA and K. The stability of the performance was measured. In addition, first-principles calculations were compared with experimental results.

2. Experimental procedures

The preparation of perovskite solar cells is shown in Figure 1 [29-32]. The FTO (F-doped Tin Oxide) substrates were ultrasonically cleaned with acetone and methanol and dried under nitrogen gas. TiO_2 precursor solution (0.15, 0.30 M) was prepared by adding 1-butanol (1 mL) to titanium diisopropoxide bis(acetylacetonate) (Sigma-Aldrich, St. Louis, MO, USA, 0.055, 0.11 mL). The 0.15 M TiO_2 precursor solution was spin-coated onto the FTO substrate at 3000 rpm for 30 s, and then the coated substrate was annealed at 125 °C for 5 min. 0.30 M TiO_2 precursor solution was spin-coated onto the TiO_2 layer at 3000 rpm for 30 s, and then the resulting substrate was annealed at 125 °C for 5 minutes. This process of forming the 0.30 M precursor layer was carried out twice. The FTO substrate was then baked at 550 °C for 30 min to form a compact TiO_2 layer. To form the mesoporous TiO_2 layer, TiO_2 paste was prepared by mixing TiO_2 powder (Aerosil, Tokyo, Japan, P-25, 200 mg) and poly(ethylene glycol) (Wako Pure Chemical Corporation, Osaka, Japan, PEG #20000 20 mg) with ultrapure water (1 mL). To this solution, acetylacetone (Wako Pure Chemical Corporation, Osaka, Japan, 20 µL) and surfactant (Sigma-Aldrich, St. Louis, MO, USA, Triton X-100, 10 µL) were added, mixed for 30 min, and then allowed to stand for 24 h to remove bubbles in the solution. The TiO_2 paste was then spin-coated on the compact TiO_2 layer at 5000 rpm for 30 s. The resulting cell was heated at 125 °C for 5 min and then annealed at 550 °C for 30 min to form a mesoporous TiO_2 layer. To prepare the perovskite compound, a mixture of CH_3NH_3I (2.4 M, Tokyo Chemical Industry, Tokyo, Japan), $PbCl_2$ (0.8 M, Sigma-Aldrich, St. Louis, MO, USA) in DMF (Nacalai Tesque, Kyoto, Japan, 0.5 mL) solution was prepared for the standard cell. Then, these perovskite solutions were spin-coated on TiO_2 at 2000 rpm for 60 s with air blow. This process was performed three times: a solution of DPPS (Osaka Gas Chemical, OGSOL SI-30-15, Osaka, Japan, 10 mg) was prepared in chlorobenzene (0.5 mL) and dropped onto the perovskite layer during the last 15 s of the third spin coating of the perovskite precursor solution [33-37]. Subsequently, annealing was performed at 200 °C in air. Spiro-OMeTAD (Sigma-Aldrich, St. Louis, MO, USA, 36.1 mg) was dissolved in chlorobenzene (Wako Pure Chemical corporation, 0.5 mL). Lithium bis(trifluoromethylsulfonyl)imide (Li-TFSI, Tokyo Chemical Industry, Tokyo, Japan, 260 mg) and FK209 (Sigma-Aldrich, St. Louis, MO, USA, 188 mg) were each added to acetonitrile (Sigma-Aldrich, St. Louis, MO, USA, 0.5 mL). Immediately before membrane formation, 4-tertbutylpyridine (Sigma-Aldrich, St. Louis, MO, USA, 18 µL), the prepared solution of Li-TFSI (10 µL), and the solution of FK209 (4 µL) were mixed at 70 °C for 30 min. The spiro-OMeTAD solution was then spin-coated on the perovskite layer at 4000 rpm for 30 seconds. All procedures were performed in air. Finally, a gold (Au) electrode was deposited to serve as the top electrode. The layer structure of the prepared solar cell is FTO/TiO_2/perovskite/spiro-OMeTAD/Au. The prepared perovskite solar cells were stored at a temperature of 22°C and humidity below 30%.

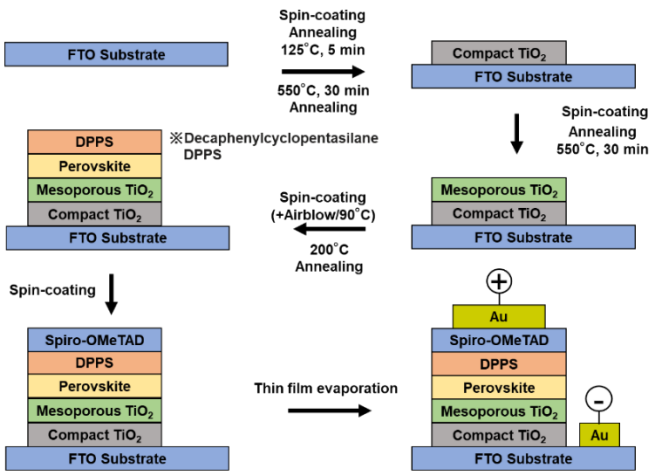

Figure 1. Schematics the processes for the PSC architectures.

3. Results and discussion

3.1. First-principles calculation

The electron distribution diagrams and density of states (DOS) of $MAPbI_3$ and Cu-doped $MAPbCuI_3$ were calculated by first-principles calculations [38-42]. $MAPbCuI_3$ increase in DOS due to the overlap of Cu 3d and I 5p orbitals near the HOMO. Indicating charge transfer from I 5p orbitals through Cu 3d orbitals. From the results, it is predicted that the short-circuit current density (J_{SC}) increases due to the easier hole migration. The calculation of the band gap (E_g) suggested that the simultaneous addition of Cu and K would increase the E_g related to the open circuit voltage (V_{OC}). E_g is the energy gap between the highest occupied molecular orbital (HOMO) and the lowest unoccupied molecular orbital (LUMO).

The cubic and crystal models doped with Cu and GA are shown in Fig. 2. From the energy calculation, the GA doped system had increase of energy, yielding unstable state, as compared to the standard system. These results suggest that the stability of the performance of the perovskite crystal is improved by the simultaneous addition of Cu and K. In the other case, the perovskite crystal with addition of GA might occur the crystal decomposition with the distortion of MA.

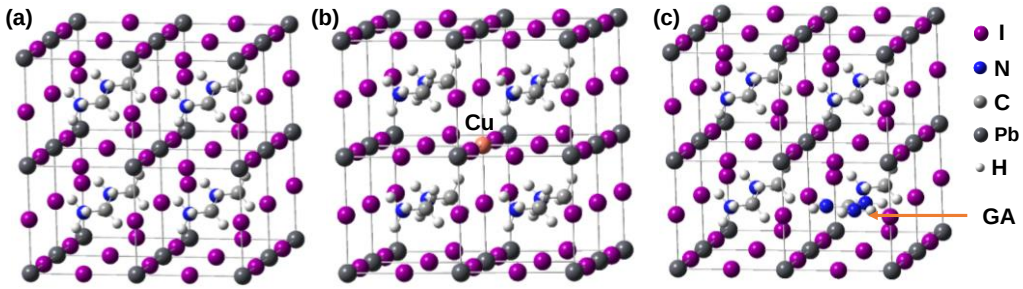

Figure 2. Crystal structures of cubic (a) $MAPbI_3$, (b) $MAPb_{0.963}Cu_{0.037}I_3$, and (c) $MA_{0.875}GA_{0.125}PbI_3$.

3.2. Device characterization

Immediately after fabrication, the current-voltage characteristic (*J-V*) curve and the external quantum efficiency (EQE) spectrum were measured. The performance of the Cu 2% + K 2% doped device was inferior to that of the standard device. The surface observation of SEM and EDX analysis showed uniform morphologies and monodispersed crystal grain in the perovskite crystals containing a slight K. The GA-doped perovskite crystal exhibited a tetragonal crystal system, consistent with calculated predictions and X-ray diffraction pattern.

The stability of conversion efficiency of the devices was investigated. The performance of the devices doped with Cu and K simultaneously maintained to be about 10.8 % after 28 days, while the performance of the standard devices was reduced by about 8.5%. The optical micrographs showed grain growth with increase of size. The XRD pattern indicate the lattice constant of the crystals was decreased by doping Cu and K.

Schematic model of atomic diffusion in the Cu, K-added perovskite crystals is illustrated in Fig. 3. It is considered that the lattice constant of the perovskite crystal was decreased by the substitution of K, which was not added immediately after the device fabrication, to the desorption position of MA with the passage of time. The simultaneous addition of Cu and K to the perovskite crystal decreased the lattice constant, yielding wide band gap related to $V_{OC,}$ as compared to those in the $MAPbI_3$ perovskite crystal.

4. Conclusion

Effects of co-addition of $CuCl_2$, KI and GAI to $MAPbI_3$ on the photovoltaic properties, microstructures and crystal structure were investigated. It was found that the devices with 2% Cu and 2% K doping had the best stability and performance with an increase in the V_{OC}, R_S and R_{Sh} parameters. The addition of K in the perovskite layer promoted the uniform crystal growth with increase of grain size while inhibiting crystal decomposition, yielding the stability of the performance.

Author Contributions: Conceptualization, A.E.; methodology, A.E., A.S. and T.O.; formal analysis, A.E., A.S. and T.O; investigation, A.E.; resources, A.E., A.S. and T.O; data curation, A.E., A.S. and T.O; writing—original draft preparation, A.E., A.S. and T.O; project administration, A.E., A.S. and T.O; funding acquisition, A.E., A.S. and T.O.

Funding: This research was supported by JSPS KAKENHI Grant Number JP 21K05261.

References

1. Kovalenko, M.V.; Protesescu, L.; Bodnarchuk, M.I. Properties and potential optoelectronic applications of lead halide perovskite nanocrystals. *Science.* **2017**, 358, 745–750, doi:10.1126/science.aam7093.
2. Umari, P.; Mosconi, E.; Angelis, F.D. Relativistic GW calculations on $CH_3NH_3PbI_3$ and $CH_3NH_3SnI_3$ perovskites for solar cell applications. *Sci. Rep*. **2014**, 3, doi:10.1038/srep04467.
3. Brivio, F.; Frost, J.M.; Skelton, J.M.; Jackson, A.J.; Weber, O.J.; Weller, M.T.; Goni, A.R.; Leguy, A.M.A.; Barnes, P.R.F.; Walsh, A. Lattice dynamics and vibrational spectra of the orthorhombic, tetragonal, and cubic phases of methylammonium lead iodide. *Phys. Rev. B* 92, **2015,** 144308, doi:10.1103/PhysRevB.92.144308.
4. Bu, T.; Li, J.; Li, H.; Tian, C.; Su, J.; Tong, G.; Ono, L.K.; Wang, C.; Lin, Z.; Chai, N.; Zhang, X-L.; Chang, J.; Lu, J.; Zhong, J.; Huang, W.; Qi, Y.; Cheng, Y-B.; Huang, F. Lead halide–template crystallization of methylamine-free perovskite for efficient photovoltaic modules. *Science.* **2021,** 372, 1327–1332, doi:10.1126/science.abh1035.
5. Ashari-Astani, N.; Meloni, S.; Salavati, A.H.; Palermo, G.; Gratzel, M.; Rothlisberger, U. Computational characterization of the dependence of halide perovskite effective masses on chemical composition and structure. *J, Phys, Chem, C*. **2017**, 121, 23886−23895, doi:10.1021/acs.jpcc.7b04898.
6. Qiao, L.; Fang, W-H.; Long, R.; Prezhdo, O.V. Photoinduced dynamics of charge carriers in metal halide perovskites from an atomistic perspective. *J. Phys. Chem. Lett.* **2020**, 11, 7066−7082, doi:10.1021/acs.jpclett.0c01687.
7. Singh, T.; Miyasaka, T. Stabilizing the efficiency beyond 20% with a mixed cation perovskite solar cell fabricated in ambient air under controlled humidity. *Adv. Energy Mater.* **2018**, 8, 1700677, doi:10.1002/aenm.201700677.
8. Chen, S.; Dai, X.; Xu, S.; Jiao, H.; Zhao, L.; Huang, J. Stabilizing perovskite-substrate interfaces for high-performance perovskite modules. *Science.* **2021**, 373, 902–907, doi:10.1126/science.abi6323.
9. Zou, Y.; Teng, P.; Xu, W.; Zheng, G.; Lin, W.; Yin, J.; Kobera, L.; Abbrent, S.; Li, X.; Steele, J.A.; Solano, E.; Roeffaers, M.B.J.; Li, J.; Cai, L.; Kuang, C.; Scheblykin, I.G.; Brus, J.; Zheng, K.; Yang, Y.; Mohammed, O.F.; Bakr, O.M.; Pullerits, T.; Bai, S.; Sun, B.; Gao, F. Manipulating crystallization dynamics through chelating molecules for bright perovskite emitters. *Nat. Commun,* **2021** 12, 4831, doi:10.1038/s41467-021-25092-7.
10. Wang, Y.; Mahmoudi, T.; Hahn, Y-B. Highly stable and Efficient Perovskite Solar Cells Based on FAMA-perovskite-Cu:NiO composites with 20.7% efficiency and 80.5% fill factor. *Adv. Energy Mater*. **2020**, 10, 2000967, doi:10.1002/aenm.202000967.
11. Oku, T.; Crystal structures of perovskite halide compounds used for solar cells. *Rev. Adv. Mater. Sci*. **2020**, 59, 264–305, doi:10.1515/rams-2020-0015.
12. Jodlowski, A.D.; Roldán-Carmona, C.; Grancini, G.; Salado, M.; Ralaiarisoa, M.; Ahmad, S.; Koch, N.; Camacho, L.; Miguel, G.d.; Nazeeruddin, M.K. Large guanidinium cation mixed with methylammonium in lead iodide perovskites for 19% efficient solar cells. *Nat. Energy*. **2017**, 12, 972–979, doi:10.1038/ s41560-017-0054-3.
13. Zhang, W.; Xiong, J.; Li, J.; Daoud, W.A. Guanidinium induced phase separated perovskite layer for efficient and highly stable solar cells. *J. Mater. Chem. A*. **2019**, 7, 9486–9496, doi:10.1039/c9ta01893j.
14. Kishimoto, T.; Suzuki, A.; Ueoka, N.; Oku, T. Effects of guanidinium addition to $CH_3NH_3PbI_{3-x}Cl_x$ perovskite photovoltaic devices. *J. Ceram. Soc. Jpn.* **2019**, *127*, 491−497, doi:10.2109/jcersj2.18214.
15. Jang, J.; Ji, S.; Grandhi, G.K.; Cho, H.B.; Im, W.B.; Park, J-U. Multimodal digital X-ray scanners with synchronous mapping of tactile pressure distributions using perovskites. *Adv. Mater*. **2021**, 33, 2008539, doi: 10.1002/adma.202008539.
16. Tang, Z.; Bessho, T.; Awai, F.; Kinoshita, T.; Maitani, M.M.; Jono, R.; Murakami, T.N.; Wang, H.; Kubo, T.; Uchida, S.; Segawa, H. Hysteresis-free perovskite solar cells made of potassium-doped organometal halide perovskite. *Sci. Rep,* **2017**, doi:10.1038/s41598-017-12436-x.
17. Alanazi, T.I.; Game, O.S.; Smith, J.A.; Kilbride, R.C.; Greenl, C.; Jayaprakash, R.; Georgiou, K.; Terrill, N.J.; Lidzey, D.G. Potassium iodide reduces the stability of triplication perovskite solar cells. *RSC Adv*. **2020**, 10, 40341, doi:10.1039/d0ra07107b.

18. Kandori, S.; Oku, T.; Nishi, K.; Kishimoto, T.; Ueoka, N.; Suzuki A. Fabrication and characterization of potassium and formamidinium-added perovskite solar cells. *J. Ceram. Soc. Jpn.* **2020,** 128 ,10, 805-811, doi:10.2109/jcersj2.20090.
19. Jiang, J.; Xu, J.; Walter, H.; Kazi, A.; Wang, D.; Wangila, G.; Mortazavi, M.; Yan, C.; Jiang, Q. The doping of alkali metal for halide perovskites. *ES Mater. Manuf*. **2020**, 7, 25-33, 25, doi:10.30919/esmm5f705.
20. Klug, M.T.; Osherov, A.; Haghighirad, A.A.; Stranks, S.D.; Brown, P.R.; Bai, S.; Wang, J.T.-W.; Dang, X.; Bulovic, V.; Snaith, H.J.; Belcher, A.M. Tailoring metal halide perovskites through metal substitution: influence on photovoltaic and material properties. *Energy Environ. Sci.* **2017**, 10, 236-246, doi:10.1039/c6ee03201j.
21. Li, Y.; Zhou, Z.; Tewari, N.; Ng, M.; Geng, P.; Chen. D.; Ko, P.K.; Qammar, M.; Guo, L.; Halpert, J.E. Progress in copper metal halides for optoelectronic applications. *Mater. Chem. Front*. **2021**, 5, 4796, doi:10.1039/d1qm00288k.
22. Karthick, S,; Hawashin, H,; Parou, N,; Vedraine, S.; Velumani, S,; Boucle, J. Copper and bismuth incorporated mixed cation perovskite solar cells by oen-step solution process. *Solar Energy*. **2021**, 218 226-236, doi:10.1016/j-solener.2021.02.053.
23. Li, M.; Wang, Z-K.; Zhuo, M-P.; Hu, Y.; Hu, K-H.; Ye, Q-Q.; Jain, S.M.; Yang, Y-G.; Gao, X-Y.; Liao, L-S. Pb–Sn–Cu Ternary organometallic halide perovskite solar cells. *Adv. Mater*. **2018**, 1800258. doi:10.1002/adma.201800258.
24. Elseman, A.M.; Shalan, A.E.; Sajid, S.; Rashad, M.M.; Hassan, A.M.; Li, M. Copper-substituted lead perovskite materials constructed with different halides for working $(CH_3NH_3)_2CuX_4$-based perovskite solar cells from experimental and theoretical view. *ACS Appl. Mater. Interfaces* **2018**, 10, 11699−11707, doi:10.1021/acsami.8b00495.
25. Ueoka, N.; Oku, T.; Suzuki, A. Effects of doping with Na, K, Rb, and formamidinium cations on $(CH_3NH_3)_{0.99}Rb_{0.01}Pb_{0.99}Cu_{0.01}I_{3-x}(Cl, Br)_x$ perovskite photovoltaic cells. *AIP Adv*. **2020**, 10, 125023, doi: 10.1063/5.0029162.
26. Ge, X.; Qu, X.; He, L.; Sun, Y.; Guan, X.; Pang, Z.; Wang, C.; Yang, L.; Wang, F.; Rosei, F. 3D low toxicity Cu–Pb binary perovskite films and their photoluminescent/photovoltaic performance. *J. Mater. Chem. A*. **2019**, 7, 27225, doi:10.1039/c9ta12736d.
27. Ueoka, N.; Oku, T. Effects of Co-addition of sodium chloride and copper (II) bromide to mixed-cation mixed-halide perovskite photovoltaic devices. *ACS Appl. Energy Mater*. **2020**, 3, 7272−7283, doi:10.1021/acsaem.0c00182.
28. Wang, K-L.; Wang, R.; Wang, Z-K.; Li, M.; Zhang, Y.; Ma, H.; Liao, L-S.; Yang, Y. Tailored phase transformation of $CsPbI_2Br$ films by copper (II) bromide for high-performance all-inorganic perovskite solar cells. *Nano Lett*. **2019**, 19, 5176-5184, doi:10.1021/acs.nanolett.9b01553.
29. Oku, T.; Zushi, M.; Imanishi, Y.; Suzuki, A.; Suzuki, K. Microstructures and photovoltaic properties of perovskite-type $CH_3NH_3PbI_3$ compounds. *Appl. Phys. Express* **2014**, *7*, 121601, doi:10.7567/APEX.7.121601.
30. Oku, T.; Ohishi, Y.; Ueoka, N. Highly (100)-oriented $CH_3NH_3PbI_3$(Cl) perovskite solar cells prepared with NH_4Cl using an air blow method. *RSC Adv.* **2018**, *8*, 10389–10395, doi:10.1039/c7ra13582c.
31. Suzuki A.; Oe M.; Oku T., Fabrication and characterization of Ni-, Co-, and Rb-incorporated $CH_3NH_3PbI_3$ perovskite solar cells, *J. Electronic Mater.* **2021**, *50*, 1980-1995. doi:10.1007/s11664-021-08759-1.
32. Oku, T. Crystal structures of perovskite halide compounds used for solar cells. *Rev. Adv. Mater. Sci.* **2020**, *59*, 264–305, doi:10.1515/rams-2020-0015.
33. Taguchi, M.; Suzuki, A.; Oku, T.; Ueoka, N.; Minami, S.; Okita, M. Effects of annealing temperature on decaphenylcyclopentasilane-inserted $CH_3NH_3PbI_3$ perovskite solar cells. *Chem. Phys. Lett.* **2019**, *737*, 136822, doi:10.1016/j.cplett.2019.136822.
34. Oku, T.; Kandori, S.; Taguchi, M.; Suzuki, A.; Okita, M.; Minami, S.; Fukunishi, S.; Tachikawa, T. Polysilane-Inserted Methylammonium Lead iodide perovskite solar cells doped with formamidinium and potassium. *Energies* **2020**, 13, 4776, doi:10.3390/en13184776.
35. Suzuki A.; Taguchi M.; Oku T.; Okita M.; Minami S.; Fukunishi S.; Tachikawa T., Additive effects of methyl ammonium bromide or formamidinium bromide in methylammonium lead iodide perovskite solar cells using decaphenylcyclopentasilane, *J. Mater. Sci.: Mater. Electron.* **2021**, *32*, 26449–26464, doi:10.1007/s10854-021-07023-w
36. Oku, T.; Taguchi, M.; Suzuki, A.; Kitagawa, K.; Asakawa, Y.; Yoshida, S.; Okita, M.; Minami, S.; Fukunishi, S.; Tachikawa, T. Effects of polysilane addition to chlorobenzene and high temperature annealing on $CH_3NH_3PbI_3$ perovskite photovoltaic devices. *Coatings* **2021**, 11, 665, doi:10.3390/coatings11060665.
37. Suzuki A.; Kitagawa K.; Oku T.; Okita M.; Fukunishi S.; Tachikawa T., Additive effects of copper and alkali metal halides into methylammonium lead iodide perovskite solar cells, *Electron. Mater. Lett.* **2021**, doi:10.1007/s13391-021-00325-5.
38. Ueoka, N.; Oku, T.; Suzuki, A. Additive effects of alkali metals on Cu-modified $CH_3NH_3PbI_{3-\delta}Cl_\delta$ photovoltaic devices. *RSC Adv.* **2019**, *9*, 24231–24240, doi:10.1039/c9ra03068a.
39. Suzuki A.; Oku T., Electronic structures and magnetic properties of transition metal doped $CsPbI_3$ perovskite compounds by first-principles calculation, *Phys. Solid State*, **2019**, *61*, 1074–1085. https://doi.org/10.1134/S1063783419060258
40. Kishimoto, T.; Oku, T.; Suzuki, A.; Ueoka, N. Additive effects of guanidinium iodide on $CH_3NH_3PbI_3$ perovskite solar cells. *Phys. Status Solidi A* **2021**, 218, 2100396. doi:10.1002/pssa.202100396.
41. Suzuki A.; Oku T., Effects of mixed-valence states of Eu-doped $FAPbI_3$ perovskite crystals studied by first-principles calculation, *Mater. Adv*., **2021**, 2, 2609-2616. https://doi.org/10.1039/D0MA00994F
42. Suzuki A.; Oku T., First-principles calculation study of electronic structures of alkali metals (Li, K, Na and Rb)-incorporated formamidinium lead halide perovskite compounds, *Appl. Surf. Sci*. **2019**, *483*, 912-921. https://doi.org/10.1016/j.apsusc.2019.04.049